

# Development of efficiency improved polymer-modified TiO<sub>2</sub> for the photocatalytic degradation of an organic dye from wastewater environment

Murugan Sangareswari<sup>1</sup> · Mariappan Meenakshi Sundaram<sup>1</sup>

Received: 31 March 2015 / Accepted: 5 October 2015 / Published online: 27 October 2015  
© The Author(s) 2015. This article is published with open access at Springerlink.com

**Abstract** In this study, the photocatalytic activity of polypyrrole-TiO<sub>2</sub> nanocomposite was studied experimentally for the degradation of methylene blue (MB) dye under simulating solar light irradiation. To improve the photocatalytic activity of TiO<sub>2</sub> under sunlight irradiation, conducting polymers such as polypyrrole (PPy) and its derivatives are generally used as photosensitizers. The PPy-TiO<sub>2</sub> nanocomposite was prepared by the chemical oxidative polymerization method. The prepared nanocomposite showed better photocatalytic activity than bare TiO<sub>2</sub> under sunlight irradiation for the degradation of MB dye. The prepared nanocomposite was subjected to characterization techniques such as SEM-EDAX, FT-IR, UV-DRS, XRD, TGA and PL spectral analysis. Different influencing operating parameters like initial concentration of dye, irradiation time, pH and amount of PPy-TiO<sub>2</sub> nanocomposite used have also been studied. The optical density of the dye degradation was measured by UV-Visible spectrophotometer. The repeatability of photocatalytic activity was also tested. A plausible mechanism was proposed and discussed on the basis of experimental results.

**Keywords** PPy-TiO<sub>2</sub> nanocomposite · Methylene blue · Sun light · Scanning Electron Microscopy · Photocatalysis

## Introduction

In current years, pollution from dye wastewater has become a severe ecological problem due to the enormous and increasing uses of a variety of dyes (Kangwansupamonkon et al. 2010). When these compounds are discharged to the major water bodies without any previous treatment, they can cause disaster to the ecological equilibrium in the environment as these molecules have carcinogenic and mutagenic properties in the direction of water organisms and thus produce treat to a human being at the end of these food chains (Muthirulan et al. 2012a, b). Methylene blue is a heterocyclic aromatic substance having IUPAC name 3,7-bis(dimethylamine)-phenothiazine-5-iumchloride with the molecular formula C<sub>16</sub>H<sub>18</sub>N<sub>3</sub>SCl. It has many uses in a selection of different fields, such as environmental science and chemistry (Eskizeybek et al. 2012). The physico-chemical properties of methylene blue (MB) dye are illustrated in Table 1.

Methylene blue dye is a cationic dye. The pzc of TiO<sub>2</sub> is 6.8. For pH values less than pH<sub>pzc</sub>, the surface becomes positively charged, and for pH values greater than pH<sub>pzc</sub> the TiO<sub>2</sub> surface will be negatively charged. Hence, it is absorbed the positively charged MB dye species easily in basic pH.

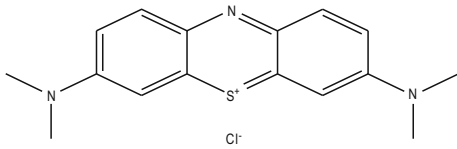
Semiconductor photocatalysis shows a potential approach for solving worldwide environmental pollution issues. Titanium dioxide (TiO<sub>2</sub>), as an important semiconductor, has been widely investigated in the photocatalytic field, due to its abnormal chemical and physical behaviours. On the other hand, the high charge recombination rate in TiO<sub>2</sub> considerably limits its photocatalytic application (Ibrahim and Halim 2008; Maeda 2012; Ochiai and Fujishima 2012; Park et al. 2013).

To develop the photocatalytic activity of TiO<sub>2</sub>, there has been significant progress in the construction of new

✉ Mariappan Meenakshi Sundaram  
drmmsundaram61@gmail.com

<sup>1</sup> Centre for Research and Post Graduate Studies in Chemistry, Ayya Nadar Janaki Ammal College (Autonomous), Sivakasi 626124, Tamil Nadu, India

**Table 1** Physico-chemical properties of MB dye

Dye	Methylene blue
Characteristics	Cationic, water soluble
Molecular formula	C <sub>16</sub> H <sub>18</sub> N <sub>3</sub> SCl
Molecular weight	319.85 g/mol
Structure	 <p>3,7-bis (dimethylamino) - phenothiazine-5-ium chloride</p>
$\lambda_{\max}$	665 nm
Applications	Redox indicator, peroxide generator, sulphide analysis, biology, photodynamic treatment of cancer

efficient materials by coupling TiO<sub>2</sub> with other organic, inorganic, polymeric materials, such as TiO<sub>2</sub>/zeolite, TiO<sub>2</sub>/activated carbon, TiO<sub>2</sub>/Al<sub>2</sub>O<sub>3</sub>, TiO<sub>2</sub>/SiO<sub>2</sub> and TiO<sub>2</sub>/polymer materials. These composites really show photocatalytic development to a certain level. Among them, TiO<sub>2</sub>/polymer composite paying more attention than others. The reason is that apart from outstanding mechanical property and large surface area, polypyrrole has electrical and electronic properties.

In recent times, some studies have been published on the combination of conductive polymers and TiO<sub>2</sub> to get better performance of UV light and sunlight activities (Muthirulan et al. 2013; Hou et al. 2011; Xu et al. 2012; Zhang et al. 2008; Denga et al. 2012; Zhang et al. 2006; Li et al. 2008; Wang et al. 2008; Kandiel et al. 2009; Wang et al. 2009). Moreover, many conjugated polymers also are efficient electron donors and good hole transporters upon visible light excitation. Therefore, conjugated polymers with large band gap inorganic semiconductors obtain awareness for optical, electronic, photocatalytic and photoelectric conversion applications.

In spite of many reward of TiO<sub>2</sub>, its photocatalytic water-splitting efficiency under solar energy is still somewhat low, mainly owing to the following reasons; First, the photo-generated electrons in the CB of TiO<sub>2</sub> can recombine with the VB holes rapidly to liberate energy in the outward appearance of blocked heat or photons; Second, the decomposition of water into hydrogen and oxygen is a chemical reaction with large positive Gibb's free energy ( $\Delta G = 237\text{kJ/mol}$ ), thus the backward reaction (recombination of hydrogen and oxygen into water) easily proceeds; Third, the band gap of TiO<sub>2</sub> is about 3.2 eV. Since UV light only accounts for in the region of 4 % of solar energy, while visible light contributes about 50 %, the lack of ability to make use of visible light confines the effectiveness of TiO<sub>2</sub> in solar photocatalytic hydrogen production.

To solve the above-mentioned trouble and to make solar photocatalytic by TiO<sub>2</sub> sufficient, constant efforts have

been made by adding electron donating organic polymer (PPy). Adding electron donors or sacrificial reagents to react with the photo-generated VB holes is an effective quantify to enhance the electron–hole separation, resulting in higher quantum efficiency. However, the disadvantage of this system is required to continuously add electron donors (organic molecules) to maintain the reaction since they will be inspired during the photocatalytic reaction. (Li et al. 2010; Ufana and Ashraf 2011; Arenas et al. 2013).

In this manuscript, effective PPy-TiO<sub>2</sub> composites have been fabricated by chemical oxidative polymerization method. The prepared PPy-TiO<sub>2</sub> nanocomposite was characterized by SEM, XRD, UV-DRS, FT-IR and PL studies. The photodegradation studies were carried out by the prepared PPy-TiO<sub>2</sub> nanocomposite. The prepared PPy-TiO<sub>2</sub> nanocomposite, a novel solar light driven catalyst PPy-TiO<sub>2</sub>, shows high photocatalytic activity as compared to TiO<sub>2</sub>.

## Experimental

### Chemicals and reagents

All these reagents are of AR grade and used without further purification. The list of chemicals is illustrated in Table 2.

**Table 2** Chemicals

Chemicals	Source
Titanium dioxide (~21 nm)	Sigma-Aldrich
Ammonium persulphate	Thomas Baker
Pyrrole (98 + %) (AR)	Alfa Aesar
Methylene blue	Qualigens
Sulphuric acid	E Merck

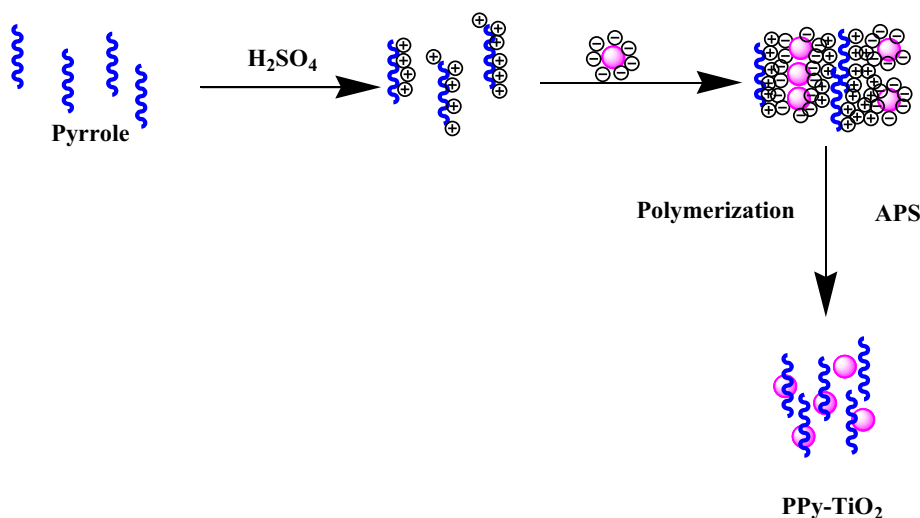
## Preparation of conductive PPy-TiO<sub>2</sub> nanocomposites

The preparation of conductive PPy-TiO<sub>2</sub> nanocomposite is illustrated in Scheme 1. Chemical oxidative polymerization of PPy was performed in the presence of negatively charged TiO<sub>2</sub> nanoparticles (different wt%, i.e. 0.5, 1.0, 1.5 and 2.0 wt%) using ammonium persulfate as an oxidant. A typical procedure is outlined: Pyrrole (5 mmol) was added to 500 ml of 0.1 M Sulphuric acid solution. Then, the TiO<sub>2</sub> nanoparticles (different wt%, i.e. 0.5, 1.0, 1.5 and 2.0) were added with continuous stirring. Then, it was kept under 5 °C cooled condition. Then, 20 ml of Ammonium persulfate solution was added drop by drop. The green coloured solution was obtained. After constant stirring, the precipitation occurred in dark colour. The obtained product was washed with distilled water to remove the remaining ammonia solution. Finally, the product was dried out at room temperature at overnight.

## Instrumental analysis

UV–visible spectrophotometer (DRS) was recorded using “SHIMADZU” model: UV 2450, FT-IR spectrum was recorded using “SHIMADZU” (Model: 8400S). The crystallographic structures of the materials were determined by high-resolution powder diffractometer model—RICH SIEFRT & CO with Cu as the X-ray source ( $\lambda = 1.5406 \times 10^{-10}$  m). The surface morphology of the sample was recorded using scanning electron microscopy (SEM-EDAX) (Model: FEG Quantum 250). The photoluminescence (LS 45) was recorded using a Perkin Elmer spectra. The thermal stability of the material was recorded using Thermogravimetric Analyser (Model : TG/DTA 6200) “SII nanotechnology”.

**Scheme 1** Synthesis of PPy-TiO<sub>2</sub> nanocomposite by chemical oxidative polymerization method



## Photodegradation studies

The photocatalytic activity of efficient PPy-TiO<sub>2</sub> nanocomposites was estimated by measuring the decolorization rates of MB. In our experiments, 50 ml of MB and 20 mg of catalysts were kept under dark room to get adsorption desorption equilibrium. Then, it suspended into sunlight irradiation. At given intervals of enlightenment, a sample of the catalyst particulate was collected and centrifuged. The supernatant was analysed by spectrophotometer (ELICO SL 207 MINI SPEC) at  $\lambda_{\max} = 665$  nm. The determined absorption was changed to concentration through the standard curve method. From that experiment, we work out the percentage removal of dye.

The amount of removal of the MB dye, in terms of percentage removal, has been calculated using the following relationship:

$$\text{Percentage removal (\%R)} = \left[ \frac{C_i - C_f}{C_i} \right] \times 100 \quad (1)$$

where  $C_i$  and  $C_f$  are the initial and final concentrations of dye (ppm) at a given time.

The reaction was carried out the time between 12.00 and 1.30 p.m. The intensity of Sun light was measured by Lux Meter (TES 1332A digital Lux meter). In this work, we did not consider the water evaporation and consequent solution concentration. The processes will be included in our future studies.

## Results and discussion

### Surface morphology of PPy-TiO<sub>2</sub> nanocomposite (SEM-EDAX)

The morphology of the composite strongly depends upon the character as well as the method of preparation. The

surface morphology of the prepared PPy-TiO<sub>2</sub> nanocomposite was examined by SEM-EDAX. Figure 1a shows the surface morphology Polypyrrole having flower like structure. Figure 1b represents that the surface morphology of TiO<sub>2</sub> is a ball-like round shape deposited on the surface of polypyrrole. Based on these conclusions in PPy-TiO<sub>2</sub> nanocomposite, the TiO<sub>2</sub> particles deposited on the outside of polypyrrole (Hongyu et al. 2010; Guoquan et al. 2011).

### FT-IR studies

The molecular structure and functional group of PPy and PPy-TiO nanocomposites (0.5, 1.0, 1.5, 2.0 wt%) were determined by FTIR spectrum. Figure 2 gives the typical FTIR spectra of PPy polymer, and the bands at 1552.15 and 1635.13 cm<sup>-1</sup> are attributed to the stretching vibrations of C=C and C=N in the phenazine ring, respectively. The peaks at 1400.22 and 1100 cm<sup>-1</sup> are attributed to the C–N stretching in the benzenoid and quinoid imine units. In

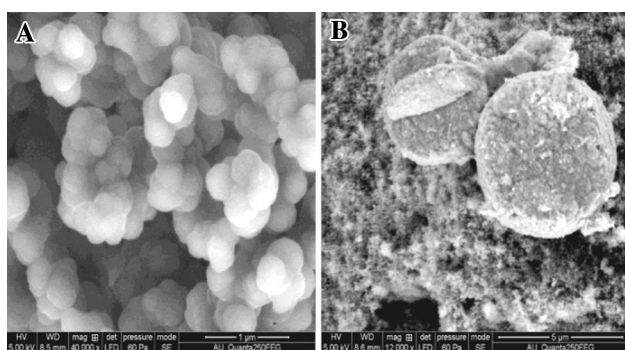


**Fig. 1** SEM images of **a** pure polypyrrole, **b** 2.0 wt% TiO<sub>2</sub>-PPy nanocomposite

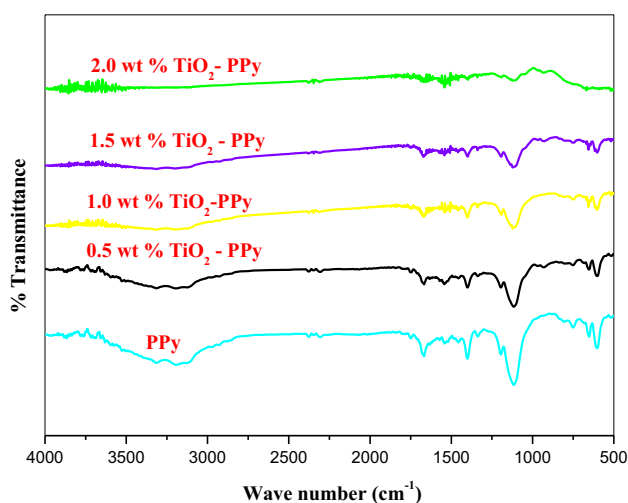


**Fig. 2** FTIR spectra of PPy, 0.5 wt% TiO<sub>2</sub>-PPy, 1.0 wt% TiO<sub>2</sub>-PPy, 1.5 wt% TiO<sub>2</sub>-PPy, 2.0 wt% TiO<sub>2</sub>-PPy

addition, the bands at 520.78 cm<sup>-1</sup> which are the description of C–H out-of plane bending vibrations of benzene nuclei of PPy. The FTIR spectra of the PPy-TiO<sub>2</sub> nanocomposites with different wt% TiO<sub>2</sub> represent the same characteristic peaks of PPy polymer. The peak in the region of 1100 cm<sup>-1</sup> is related with vibrational modes of N=Q=N (Q refers to the pyrrole ring), representing that PPy is formed in the composite. But the stretching is decreased with the increase in the loading amount of TiO<sub>2</sub>. The results of FTIR spectra of PPy agree well with the earlier reports (Xiaofang et al. 2006; Deivanayaki et al. 2012; Mi et al. 2009; Chougulea et al. 2012, 2013; Chatterjee et al. 2013; Etelino et al. 2013; Juraj et al. 2013).

### UV–vis DRS studies of PPy-TiO<sub>2</sub> nanocomposite

The optical properties of PPy-TiO<sub>2</sub> nanocomposites investigated by UV-DRS spectroscopy are shown in Fig. 3a. The band gap energies of PPy-TiO<sub>2</sub> can be estimated from the wavelength values equivalent to the junction point of the perpendicular and parallel parts of the spectra.

From that spectra, the polymer expands the absorption range of the TiO<sub>2</sub> from 400 nm to over 550 nm. In fact, the spectra of PPy-TiO<sub>2</sub> were the spectra of polymer PPy adsorbed onto the surface of the powders. It is an essential condition for photo-sensitization that the photosensitizer be adsorbed onto the surface of semiconductor. PPy-TiO<sub>2</sub> seemed to be capable of responding to visible light.

The position of the fundamental absorption edge of PPy-TiO<sub>2</sub> is determined using the equation:

$$(\alpha h\nu)^2 = A(h\nu - E_g)^n \quad (2)$$

where  $\alpha$ ,  $h$ ,  $\nu$ ,  $E_g$  and  $A$  are the absorption coefficients, plank constant, light frequency, band gap and a constant, respectively. The  $n$  value depends on the transition characteristics. The  $E_g$  value can be approximated by extrapolating the straight portion of the  $(\alpha h\nu)^2 - (h\nu)$  plot shown in Fig. 3b. The obtained  $E_g$  value occurs between 2.22 and 2.23 e V for PPy-TiO<sub>2</sub>, respectively. The band gap value of 2.0 wt% TiO<sub>2</sub>-PPy nanocomposite was smaller when compared to other components as shown in Table 3. The band gap values estimated are somewhat smaller than the reported values which can be accredited to wide particle size distribution and surface defects (Rohit et al. 2013).

### X-ray diffraction pattern of PPy-TiO<sub>2</sub> nanocomposite

The crystallographic construction of obtained PPy-TiO<sub>2</sub> nanocomposite was evidenced by XRD measurements. Figure 4a shows the XRD pattern of TiO<sub>2</sub> and Fig. 4b shows the XRD pattern of PPy/TiO<sub>2</sub> nanocomposites. The

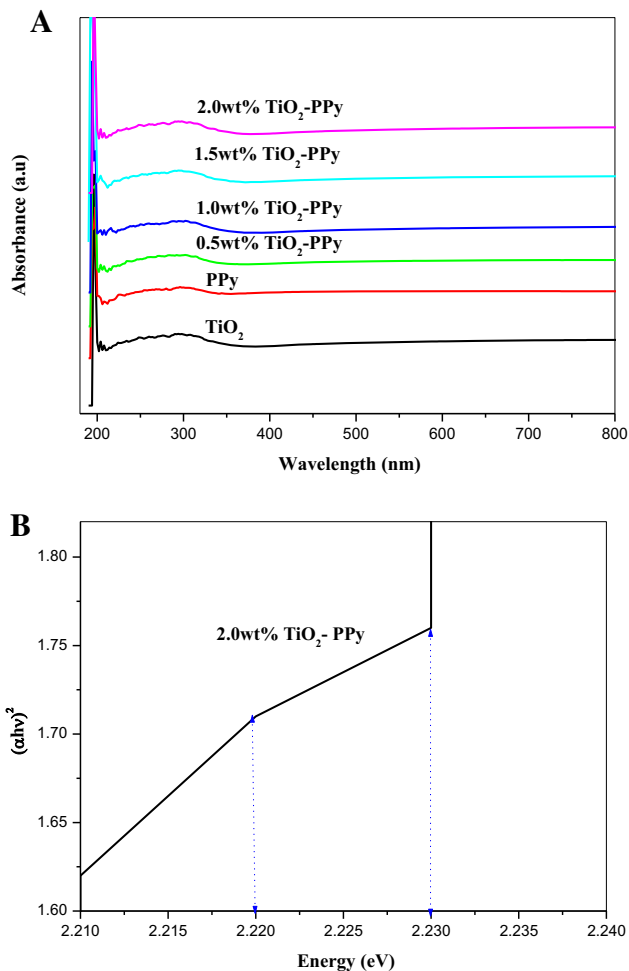


**Fig. 3** a UV-DRS spectra of PPy-TiO<sub>2</sub> nanocomposite. b Plots of the  $(xhv)^2$  vs photon energy  $(hv)$  for PPy-TiO<sub>2</sub> nanocomposite

**Table 3** Calculated band gap values for other components

Catalyst	Band gap (eV)
TiO <sub>2</sub>	3.2
PPy	2.4
0.5 wt% TiO <sub>2</sub> -PPy	3.0
1.0 wt% TiO <sub>2</sub> -PPy	2.9
1.5 wt% TiO <sub>2</sub> -PPy	2.6

XRD peaks denote the arrangement of PPy-TiO<sub>2</sub> nanocomposite. The respected peaks occur at 25.3°, 26.2°, 36.0°, 38.2°, 48.9°, 54.3°, 56.6°, 63.1°, 69.9°. In addition, it can be prominent due to the TiO<sub>2</sub> deposited on the surface of polypyrrole (Hasani and Hossein 2013; Yucheng et al. 2013).

The mean crystalline sizes of PPy-TiO<sub>2</sub> nanocomposites are designed using Scherrer's formula:

$$D_{\text{Scherrer}} = k\lambda/\beta \cos \Theta$$

where  $\lambda$  is the wavelength of the X-ray radiation ( $\lambda = 1.54 \times 10^{-9}$  nm), and  $k$  is the Scherrer constant ( $k = 0.89$ )

$\Theta$  is the diffraction angle and  $\beta$  is the line width at half-maximum height of the most intense peak. Based on the XRD results, the crystalline range of PPy-TiO<sub>2</sub> nanocomposites was in the order of 10–20 nm. The results are in good agreement with the SEM images.

### Photoluminescence spectra

To study the cause for the higher photocatalytic activity of PPy-TiO<sub>2</sub> nanocomposites, PL spectra of samples have been taken, as shown in Fig. 5. The rate of recombination of  $e^-/h^+$  pairs may also be a key factor disturbing the photoactivity of TiO<sub>2</sub>. Probably, the TiO<sub>2</sub> photocatalysts show a broad PL emission band. The peak intensities of the PL spectra of PPy-TiO<sub>2</sub>, demonstrating that the electron—hole recombination rate of self—trapped excitation in TiO<sub>2</sub>, are reduced by the introduction of PPy. The significant PL quenching of TiO<sub>2</sub> can be observed after combination with PPy, representing the efficient transfer of photo-generated electron from the TiO<sub>2</sub> to PPy, most important to the enhanced photocatalytic activity of the PPy/TiO<sub>2</sub> nanocomposites (Wang et al. 2010).

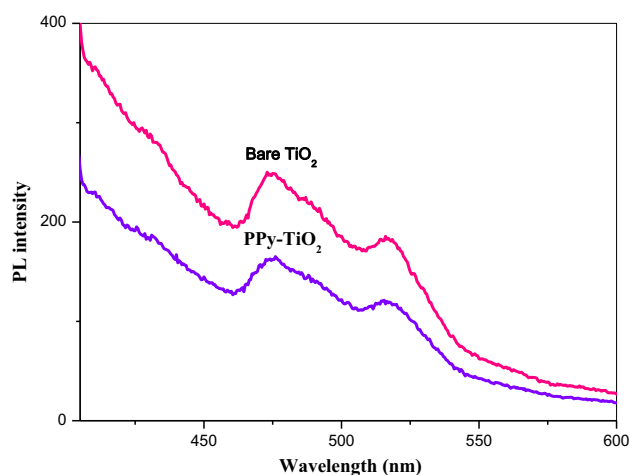
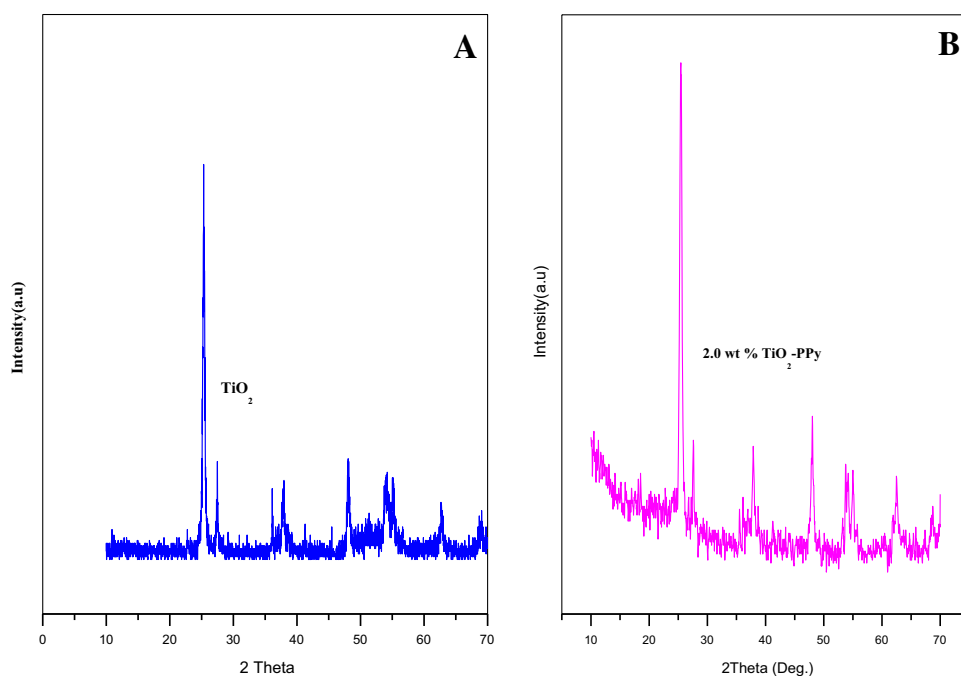
### Thermogravimetric analysis

Figure 6 displays the thermogravimetric analysis of Pure PPy, 1.0 wt% TiO<sub>2</sub>-PPy and 2.0 wt% TiO<sub>2</sub>-PPy nanocomposites under N<sub>2</sub> atmosphere with the heating rate 20 °C/min. As observed from Fig. 6, it demonstrates that the thermal stability of 2.0 wt% TiO<sub>2</sub>-PPy is much advanced than that of other composites in the temperature range of 30–800 °C. The first weight loss occurred at 100 °C due to the evaporation of remaining water molecule. The second weight loss occurs between 110 and 250 °C. This demonstrates the structural decay of PPy. Finally, the third weight loss occurs at 250–730 °C. This is due to the skeletal degradation of PPy. In contrast, 2.0 wt% TiO<sub>2</sub>-PPy nanocomposites have greater thermal stability than other two nanocomposites. The thermogram shows that the TiO<sub>2</sub> nanoparticle lost about 11.9 % weight owing to the loss of polymer coatings on the surface of the nanoparticle.

### Effect of concentration of dye

The outcome of initial concentration of Methylene Blue dye on the photocatalytic activity of photocatalysts (TiO<sub>2</sub> and PPy-TiO<sub>2</sub> nanocomposites) was carried out under solar light irradiation within the concentration range of

**Fig. 4** XRD spectra of **a**  $\text{TiO}_2$ , **b** PPy- $\text{TiO}_2$  nanocomposite



**Fig. 5** PL spectra of **a** PPy- $\text{TiO}_2$  nanocomposite, **b**  $\text{TiO}_2$

10–60 ppm and constant amount of catalyst and irradiation time and the results are shown in Fig. 7. These results indicated that PPy- $\text{TiO}_2$  nanocomposites photocatalyst showed a high efficiency for the photocatalytic degradation of MB in the presence of solar light irradiation than  $\text{TiO}_2$ .

When increasing the dye concentration from 10 to 20 ppm, the percentage decoloration of MB dye was decreased at 90–5 %. Finally, the degradation quickly decreases for 60 ppm (25 %). This may be due to:

1. higher dye concentration might serve as an inner filter shunting the photons away from the catalyst surface;
2. non-availability of oxidative free radicals;

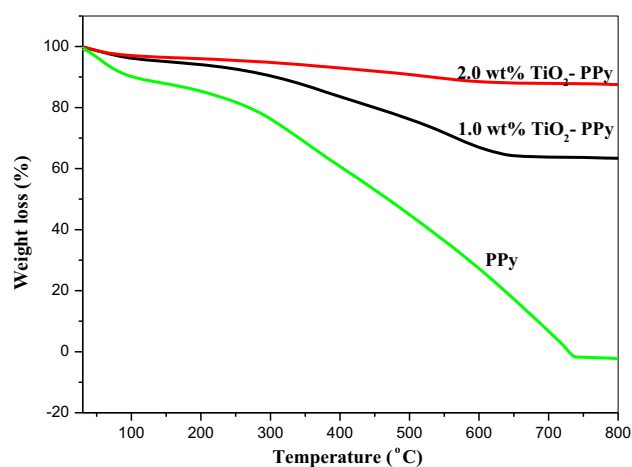


**Fig. 6** TGA/DTA spectrum for 2.0 wt%  $\text{TiO}_2$ -PPy nanocomposite

3. inverse effect is explained that if the dye concentration increases in the treating solution, large amount of dye molecules is adsorbed on catalyst surface active site. The surface active sites to contribute in the degradation reaction will help to enlarge the degradation efficiency. Due to the increase in dye concentration, there is no space for the formation of  $\text{OH}\cdot$  radicals. So at last there is a drop in degradation efficiency. Hydroxyl radical is the strongest oxidizing agent promoting the degradation rate. According to the Beer-Lambert law, as the initial dye concentration increases, the pathway distance end to end of photon incoming the solution decreases consequently resulting



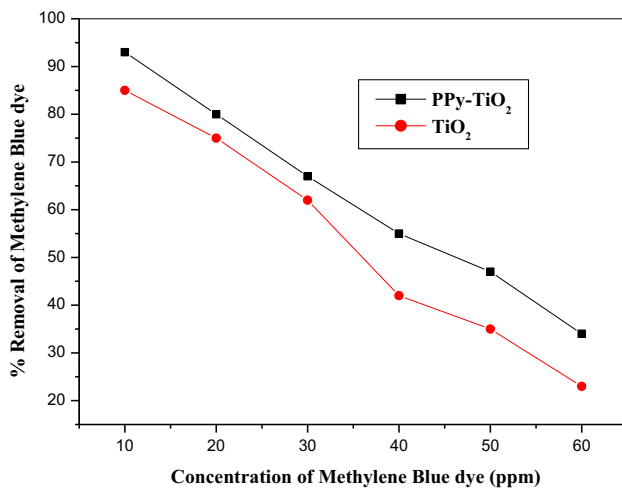


**Fig. 7** Effect of initial concentration on the photodegradation of MB dye on PPy-TiO<sub>2</sub> nanocomposite and TiO<sub>2</sub>

in lower photo degradation rate (Zhao et al. 2012; Wang et al. 2012; Selvam et al. 2007).

### Effect of dose variation

The influence of dose on the degradation of Methylene Blue has been investigated by PPy-TiO<sub>2</sub> nanocomposite. This percentage removal of dye using PPy-TiO<sub>2</sub> nanocomposites was higher than TiO<sub>2</sub> (Fig. 8). The increase in the efficiency seems to be due to the increase in the whole surface area, namely the number of active sites obtainable for the photo catalytic reaction as the quantity of photo catalyst increased. When photocatalyst is added in excess, the degradation of dye molecules remains constant.

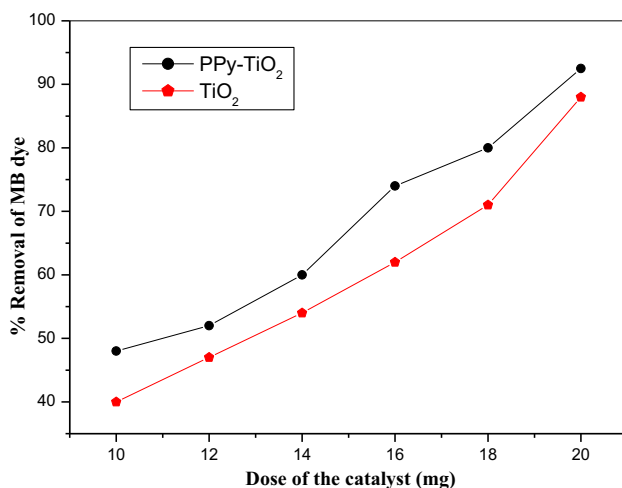


**Fig. 8** Effect of dose of the catalysts on the photodegradation of MB dye on PPy-TiO<sub>2</sub> nanocomposite and TiO<sub>2</sub>

The reason for this is the decreased light penetration, the increased light scattering and the slaughter in surface area occasioned by agglomeration at high solid concentration (Baruah et al. 2010).

### Effect of time variation

The degradation of methylene blue was exponential with time. The degradation rate constant  $k$  for methylene blue was obtained from the plot in Fig. 9 using

$$\ln\left(\frac{C_0}{C_f}\right) = kt \quad (3)$$

where  $C_0$  and  $C_f$  are the initial and final concentrations of dye and  $t$  is the irradiation of time.

The degradation rate constants are similar for both the sample with decayed methylene blue fraction of 93 % leading to enlightenment for 90 min (Kansal et al. 2007).

UV-vis absorption spectrum of MB with different reaction time under solar light irradiation in the presence of PPy-TiO<sub>2</sub> nanocomposites is illustrated in Fig. 10. Solar light irradiation leads to decreases in absorbance in MB in the presence of PPy-TiO<sub>2</sub> nanocomposites and the decrease of the absorption intensities indicated that the dye has been degraded. As can be seen in figure, the departure of the distinguishing band of MB dye at 665 nm after 90 min under solar light irradiation indicates that Methylene Blue has been degraded completely.

The value of  $\ln(C_0/C_f)$  is plotted against time (in min) and the plots are found to be linear. From the slope, the rate constants were considered for the degradation of MB dye in the presence and absence of PPy. The pseudo first-order rate constant ( $k \text{ min}^{-1}$ ) values of TiO<sub>2</sub> and PPy-TiO<sub>2</sub> system can be found out from the Fig. 9. The degradation efficiency of the MB dye PPy-TiO<sub>2</sub> nanocomposite is higher than that of TiO<sub>2</sub> as shown in Fig. 11.

### Effect of pH variation

To study the effect of pH on the decolorization efficiency, experiments were carried out at various pH values, ranging from 3 to 11 for constant dye concentration (10 ppm) and catalysts loading (Fig. 12). It has been experimental that the decolorization efficiency increases with increasing pH exhibiting a maximum rate of degradation at pH 11 and 9. The zero point charge for TiO<sub>2</sub> is 6.25. The pH increases from 7 to 11. The plane of the catalyst will become negatively charged. So the cationic dye (MB) easily attached to the catalyst surface. Finally, the percentage removal of dye increased. In contrast, at acidic condition the degradation efficiency will be decreased (Madhusudhana et al. 2012).

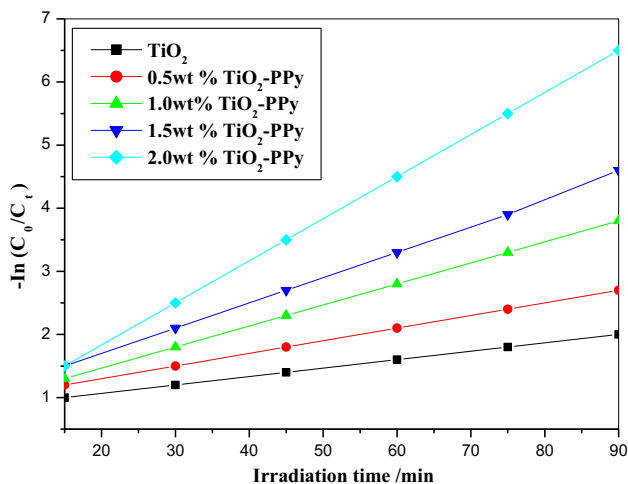


**Fig. 9** Apparent first-order linear transforms— $-\ln(C_0/C_t)$  vs.  $t$  of MB dye (dye concentration: 10 ppm) and (catalyst dose:  $0.4 \text{ g/l}^{-1}$ )

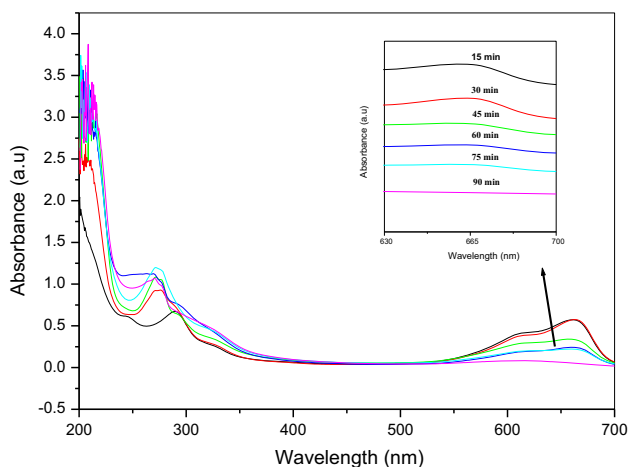


**Fig. 10** UV-vis absorption spectra of MB dye degradation using PPy-TiO<sub>2</sub> nanocomposite under solar light with different intervals of time [15, 30, 45, 60, 75, 90]

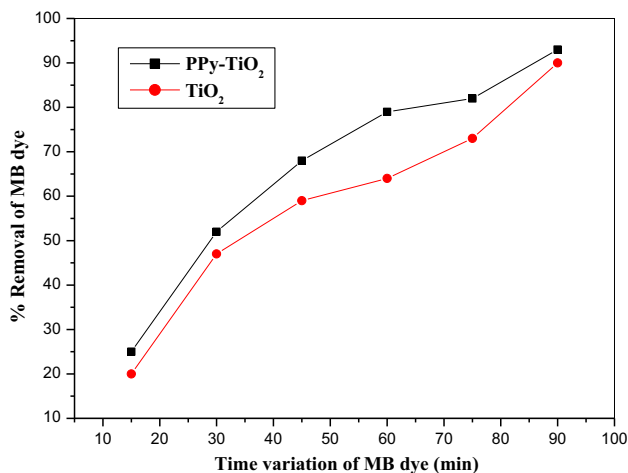


**Fig. 11** Effect of time variation on the photodegradation of MB dye on PPy-TiO<sub>2</sub> nanocomposite and TiO<sub>2</sub>

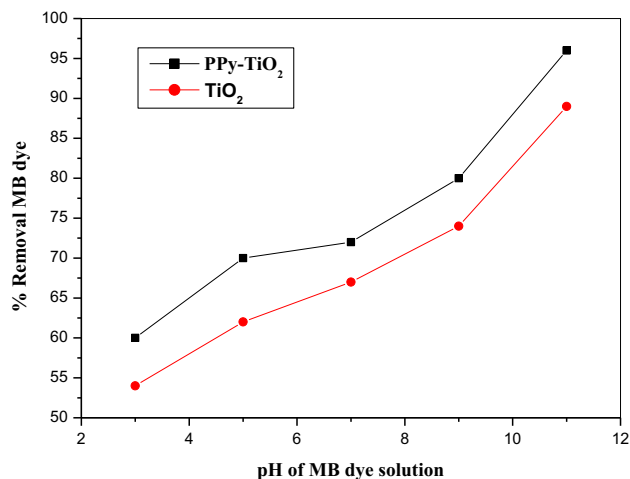


**Fig. 12** Effect of pH variation on the photodegradation of MB dye on PPy-TiO<sub>2</sub> nanocomposite and TiO<sub>2</sub>

## Mechanism

Photocatalytic mechanism of PPy-TiO<sub>2</sub> nanocomposites can be described as below. The photocurrent values obtained from PPy to TiO<sub>2</sub> nanocomposite are higher than TiO<sub>2</sub>. PPy is a p-type narrow band gap semiconductor when compared with other inorganic semiconductors (TiO<sub>2</sub>, SrTiO<sub>3</sub>, ZnO) having n-type narrow band gap semiconductor. The lowest vacant molecular orbital level of PPy is positioned in an actively higher location than the conduction band edge of TiO<sub>2</sub>. Consequently, when the system was illuminated, the excited electrons of PPy in the highest engaged molecular orbital level could move to the LUMO level, then these electrons could be transferred into the conduction band of the TiO<sub>2</sub>. Thus, more and extra photo energized electrons formed in TiO<sub>2</sub> and the combination of the semiconductors (*p-n* junction) should have a beneficial role in getting better charge separation. As a result, this scheme delivers important photo responses in this intersection.

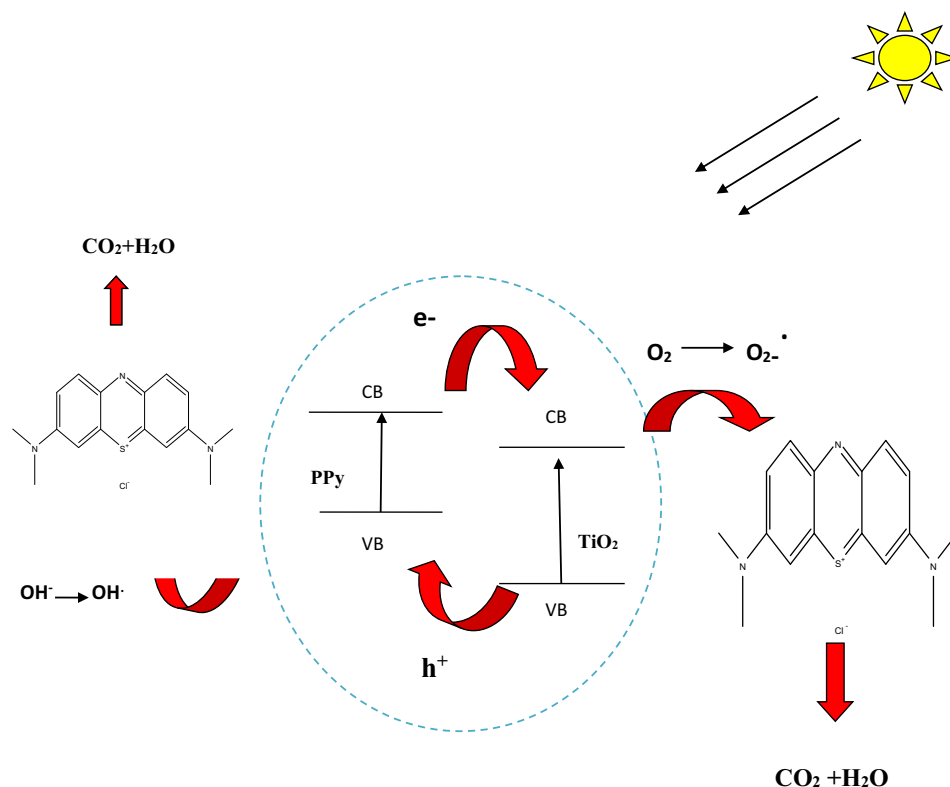
The above-discussed mechanism is illustrated in Scheme 2.

## Reuse of catalysts

The reproducibility of the photocatalytic degradation activity of a 0.02 g sample PPy-TiO<sub>2</sub> nanocomposite performed on a 10 ppm MB dye solution (50 ml) is expressed as the number of cycles, where the photocatalytic degradation of PPy-TiO<sub>2</sub> nanocomposite was reduced from 93 % on the first usage to 82, 29 and 20 % after the second, third and fourth cycles of reuse, respectively. This reduced dye photodegradation activity is in accord with the appearance of recycled PPy-TiO<sub>2</sub> nanocomposite, which was clearly



**Scheme 2** Schematic illustration on the photodegradation mechanism of MB dye on PPy-TiO<sub>2</sub> nanocomposite under solar irradiation



changed in the morphology of the PPy-TiO<sub>2</sub> nanocomposites due to the photodegradation.

## Conclusions

PPy-TiO<sub>2</sub> nanocomposite was effectively prepared by the chemical oxidative polymerization method. The results from SEM analysis consistently specify that the TiO<sub>2</sub> has been deposited on Polypyrrole atmosphere. The FT-IR results show the major functional group present in PPy-TiO<sub>2</sub> nanocomposites. The UV-vis diffuse reflectance spectra confirm that the tailored catalyst immersed more photons under visible light irradiation. The TGA spectra indicate the thermal stability of PPy-TiO<sub>2</sub> nanocomposites. The MB dye was effectively degraded by PPy-TiO<sub>2</sub> nanocomposite under solar light irradiation. The fraction removal of dye degradation was higher (93 %) in PPy-TiO<sub>2</sub> nanocomposite than TiO<sub>2</sub>.

**Acknowledgments** The authors thank the University Grants Commission, New Delhi for the Financial support in the form of Major Research Project (MRP) Grant. The authors also thank Ayya Nadar Janaki Ammal College, Sivakasi for providing laboratory facilities.

**Open Access** This article is distributed under the terms of the Creative Commons Attribution 4.0 International License (<http://creativecommons.org/licenses/by/4.0/>), which permits unrestricted use, distribution, and reproduction in any medium, provided you give

appropriate credit to the original author(s) and the source, provide a link to the Creative Commons license, and indicate if changes were made.

## References

- Arenas MC, Fernando Rodríguez-Núñez L, Domingo R, Omar Martínez A, Martínez-Alonso C, Castaño VM (2013) Simple one-step ultrasonic synthesis of anatase titania/polypyrrole nanocomposites. *Ultrason Sonochem* 20:777–784
- Baruah S, Jaisai M, Imani R, Nazhad M, Dutta J (2010) Photocatalytic paper using zinc oxide nanorods. *Sci Technol Adv Mater* 11:1–7
- Chatterjee S, Shit A, Nandi AK (2013) Nanochannel morphology of polypyrrole-ZnO nanocomposites towards dye sensitized solar cell application. *J Mater Chem A* (1):12302–12309
- Chougulea MA, Dalavib DS, Mali S, Patilb PS, Moholkarb AV, Agawanec GL, Kimc JH, Shashwati S, Patila VB (2012) Novel method for fabrication of room temperature polypyrrole-ZnO nanocomposite NO<sub>2</sub> sensor. *Measurement* S0263-22410, 0193-5
- Chougule MA, Khuspe GD, Shashwati S, Patil VB (2013) Polypyrrole-ZnO nanohybrids: effect of CSA doping on structure, morphology and optoelectronic properties. *Appl Nanosci* (3):423–429
- Deivanayaki S, Ponnuswamy V, Jayamurugan P, Ashokan S (2012) The structure and properties of polypyrrole/titaniumdioxide nanospheres of various dopant percentages by Chemical oxidation method. *Elixir Polymer* 49B:10182–10185
- Denga F, Li Y, Luob X, Lixia Y, Tu X (2012) Preparation of conductive polypyrrole/TiO<sub>2</sub> nanocomposite via surface molecular imprinting technique and its photocatalytic activity under

- simulated solar light irradiation. *Colloid Surf A: Physicochem Eng Aspects* 395:183–189
- Eskizeybek V, Fahriyesari B, Gulce H, Gulce A, Ahmet A (2012) Preparation of the new polyaniline/ZnO nanocomposite and its photocatalytic activity for degradation of MB and MG dyes under UV and natural sunlights irradiations. *Appl Catal B: Environ* 119–120:197–206
- Etelino F, Melo D, Kleber G, Alves B, Severinon A, Celso J, de Melo P (2013) Synthesis of fluorescent PVA/polypyrrole-ZnO nanofibers. *J Mater Sci* 48:3652–3658
- Guoquan Z, Shuai W, Sha Z, Lei F, Guohua C, Fenglin Y (2011) Oxidative degradation of azo dye by hydrogenperoxide electro-generated in situ on anthraquinonemonosulphonate/polypyrrole composite cathode with heterogeneous CuO/ $\gamma$ -Al<sub>2</sub>O<sub>3</sub> catalyst. *Appl Catal B: Environ* 106:370–378
- Hasani T, Hossein E (2013) Removal of Cd (II) by using polypyrrole and its nanocomposites. *Synth Met* 175:15–20
- Hongyu M, Xiaogang Z, Youlong X, Fang X (2010) Synthesis, characterization and electrochemical behavior of polypyrrole/carbon nanotube composites using organometallic-functionalized carbon nanotubes. *Appl Surf Sci* 256:2284–2288
- Hou J, Cao R, Jiao S, Zhu H, Kumar RV (2011) PANI/Bi<sub>12</sub>TiO<sub>20</sub> complex architectures: controllable synthesis and enhanced visible-light photocatalytic activities. *Appl Catal B: Environ* 104:399–406
- Ibrahim UG, Halim AA (2008) Heterogeneous photocatalytic degradation of organic contaminants over titanium dioxide: a review of fundamentals, progress and problems. *J Photochem Photobiol C: Photochem Rev* 9:1–12
- Juraj D, Martin K, Gabriela B, Martin K, Iva M (2013) Electrochemical fabrication and characterization of porous silicon/polypyrrole composites and chemical sensing of organic vapors. *Int J Electrochem Sci* 8:1559–1572
- Kandiel TA, Dillert R, Bahnemann DW (2009) Enhanced photocatalytic production of molecular hydrogen on TiO<sub>2</sub> modified with Pt: polypyrrole nanocomposites. *J Photochem Photobiol Sci* 8:683–690
- Kangwansupamonkon W, Jitbumpot W, Sudakiatkamjornwong C (2010) Photocatalytic efficiency of TiO<sub>2</sub>/poly[acrylamide-co-(acrylic acid)] composite for textile dye degradation. *Polym Degrad Stab* 95:1894–1902
- Kansal SK, Singh M, Sud D (2007) Studies on photodegradation of two commercial dyes in aqueous phase using different photocatalyst. *J Hazard Mater* 141:581–590
- Li XY, Wang DS, Cheng GX, Luo QZ, An J, Wang YH (2008) Preparation of polyaniline-modified TiO<sub>2</sub> nanoparticles and their photocatalytic activity under visible light. *Appl Catal B: Environ* 81:267–273
- Li Q, Zhang C, Li J (2010) Photocatalysis and wave-absorbing properties of polyaniline/TiO<sub>2</sub> microbelts composite by in situ polymerization method. *Appl Surf Sci* 257:944–948
- Madhusudhana N, Yogendra K, Mahadevan M (2012) A comparative study on photocatalytic degradation of violet GL2B azo dye using CaO and TiO<sub>2</sub> nanoparticles. *Int J Eng Res Appl* 2(5):1300–1307
- Maeda K (2012) Photocatalytic water splitting using semiconductor particles: history and recent developments- Invited review. *J Photochem Photobiol C: Photochem Rev* 12:237–268
- Mi O, Ru B, Yi X, Cheng Z, Chun MA, Man W, Hong-zheng C (2009) Fabrication of polypyrrole/TiO<sub>2</sub> nanocomposite via electrochemical process and its photoconductivity. *Trans Non-ferrous Met Soc China* 19:1572–1577
- Muthirulan P, Meenakshi Sundaram M, Kannan N (2012a) Beneficial role of ZnO photocatalyst supported with porous activated carbon for the mineralization of alizarin cyanin green dye in aqueous solution. *J Adv Res*. doi:10.1016/j.jare.2012.08.005
- Muthirulan P, Nirmala Devi C, Meenakshi Sundaram M (2012b) Synchronous role of coupled adsorption and photocatalytic degradation on CAC-TiO<sub>2</sub> composite generating excellent mineralization of alizarin cyanine green dye in aqueous solution. *Arab J Chem* 1:1–7
- Muthirulan P, Kannan Nirmala Devi C, Meenakshi Sundaram M (2013) Facile synthesis of novel hierarchical TiO<sub>2</sub>@Poly(o-phenylenediamine) core-shell structures with enhanced photocatalytic performance under solar light. *J Environ Chem Eng* 1:620–627
- Ochiai T, Fujishima A (2012) Photoelectrochemical properties of TiO<sub>2</sub> photocatalyst and its applications for environmental purification-invited review. *J Photochem Photobiol C: Photochem Rev* 13:247–262
- Park H, Park Y, Kim W, Choi W (2013) Surface modification of TiO<sub>2</sub> photocatalyst for environmental applications: invited review. *J Photochem Photobiol C: Photochem Rev* 15:1–20
- Rohit B, Madhulika S, Bahadur D (2013) Visible light-driven nanocomposites (BiVO<sub>4</sub>/CuCr<sub>2</sub>O<sub>4</sub>) for efficient degradation of organic dye+. *Dalton Trans* 42(19):6736–6744
- Selvam K, Muruganandham M, Muthuvel I, Swaminathan M (2007) The influence of inorganic oxidants and metal ions on semiconductor sensitized photodegradation of 4-fluorophenol. *J Chem Eng* 128:51–57
- Ufana R, Ashraf SM (2011) Semi-conducting poly(1-naphthylamine) nanotubes: a pH independent adsorbent of sulphonate dyes. *Chem Eng J* 174:546–555
- Wang DS, Wang YH, Li XY, Luo QZ, An J, Yue JX (2008) Sunlight photocatalytic activity of polypyrrole: TiO<sub>2</sub> nanocomposites prepared by 'insitu' method. *Catal Commun* 9(1162–1166):7
- Wang D, Zhang J, Luo Q, Li X, Duan Y, An J (2009) Characterization, photocatalytic activity of poly(3-hexylthiophene)-modified TiO<sub>2</sub> for degradation of methyl orange under visible light. *J Hazard Mater* 169:546–550
- Wang Y, Shi R, Lin J, Zhu Y (2010) Significant photocatalytic enhancement in methylene blue degradation of TiO<sub>2</sub> photocatalysts via grapheme-like carbon in situ hybridisation. *Appl Catal B: Environ* 100:179–183
- Wang WS, Wang DH, Qu WG, Lu LQ, Xu AW (2012) Large ultrathin anatase TiO<sub>2</sub> nanosheets with exposed 001 facets on grapheme for enhanced visible light photocatalytic activity. *J Phys Chem C* 116:19893–19901
- Xiaofang L, Qidong Z, Xin LC, Dajun W, Wanjin Z, Wang C, Wei Y (2006) Preparation and characterization of polypyrrole/TiO<sub>2</sub> coaxial nanocables. *Macromol Rapid Commun* 27:430–434
- Xu S, Gu L, Yang KH, Song Y, Jiang L, Dan Y (2012) The influence of the oxidation degree of poly(3-hexylthiophene) on the photocatalytic activity of poly(3-hexylthiophene)/TiO<sub>2</sub> composites. *Sol Energy Mater Sol Cells* 96:286–291
- Yucheng Y, Junwei W, Jianhong W, Xiong R, Shi J, Chun-Xu P (2013) Polypyrrole-decorated Ag-TiO<sub>2</sub> nanofibers exhibiting enhanced photocatalytic activity under visible light illumination. *ACS Appl Mater Interfaces* 5(13):6201–6207
- Zhang L, Liu P, Su Z (2006) Preparation of PANI/TiO<sub>2</sub> nanocomposites and their solidphase photocatalytic degradation. *Polym Degrad Stab* 91:2213–2219
- Zhao D, Sheng G, Chen C, Wang X (2012) Enhanced photocatalytic degradation in methylene blue under visible irradiation on grapheme@TiO<sub>2</sub> dyade structure. *Appl Catal B: Environ* 111:303–308